Influence of neutron and gamma-ray irradiations on rad-hard optical fiber

A. Morana,[1,*] S. Girard,[1] M. Cannas,[2] E. Marin,[1] C. Marcandella,[3] P. Paillet,[3] J. Périsse,[4] J.-R. Macé,[5] R. Boscaino,[2] B. Nacir,[6] A. Boukenter,[1] and Y. Ouerdane[1]

[1] *Laboratoire H. Curien, UMR CNRS 5516, Université Jean Monnet, 18 rue du Pr. Benoît Lauras F-42000, Saint-Etienne, France*

[2] *Dipartimento di Fisica e Chimica, Università di Palermo, via Archirafi 36, I-90123 Palermo, Italy*

[3] *CEA, DAM, DIF, F-91297 Arpajon, France*

[4] *Areva NP, 10 rue Juliette Récamier, F-69456 Lyon Cedex 06, France*

[5] *Areva, Tour Areva,1 place Jean Millier, F-92084 Paris La défense Cedex, France*

[6] *Centre National de l'Energie, des Sciences et des Techniques Nucléaires, Maamoura, Morocco*

**adriana.morana@univ-st-etienne.fr*

Abstract: We investigated point defects induced in rad-hard Fluorine-doped optical fibers using both a mixed source of neutrons (fluences from 10^{15} to 10^{17} n/cm^2) and γ-rays (doses from 0.02 to 2 MGy) and by a γ-ray source (dose up to 10 MGy). By combining several complementary spectroscopic techniques such as radiation-induced attenuation, confocal micro-luminescence, time-resolved photo-luminescence and electron paramagnetic resonance, we evidenced intrinsic and hydrogen-related defects. The comparison between the two irradiation sources highlights close similarities among the spectroscopic properties of the induced defects and the linear correlation of their concentration up to 10^{16} n/cm^2. These results are interpreted on the basis of the generation processes of defects from precursors sites, that are common to both γ-rays and neutrons. In contrast, the highest neutron fluence (10^{17} n/cm^2) causes peculiar effects, such as the growth of a photoluminescence and variations of the spectral and decay properties of the emission related with nonbridging oxygen hole centers, that are likely due to silica network modification.

OCIS codes: (060.2310) Fiber optics; (350.5610) Radiation; (300.6280) Spectroscopy, Fluorescence and luminescence; (300.1030) Absorption.

References and links

1. S. Girard, J. Kuhnhenn, A. Gusarov, B. Brichard, M. Van Uffelen, Y. Ouerdane, A. Boukenter and C. Marcandella, "Radiation effects on silica-based optical fibers: recent advances and future challenges," IEEE Trans. Nucl. Sci. **60**(3), 2015–2036 (2013).
2. L. Skuja, M. Hirano, H. Hosono and K. Kajihara, "Defects in oxide glasses," Phys. Stat. Sol. **C2**(1), 15–24 (2005).

#230868 - $15.00 USD Received 27 Jan 2015; revised 11 Mar 2015; accepted 17 Mar 2015; published 30 Mar 2015

3. G. Cheymol, H. Long, J. F. Villard and B. Brichard, "High level gamma and neutron irradiation of silica optical fibers in CEA OSIRIS nuclear reactor," IEEE Trans. Nucl. Sci. **55**(4), 2252–2258 (2008).
4. B. Brichard, A. Fernandez Fernandez, H. Ooms, P. Borgermans and F. Berghmans, "Dependence of the POR and NBOHC defects as function of the dose in hydrogen-treated and untreated KU1 glass fibers," IEEE Trans. Nucl. Sci. **50**(6), 2024–2029 (2003).
5. A. Morana, M. Cannas, S. Girard, A. Boukenter, L. Vaccaro, J. Périsse, J.-R. Macé, Y. Ouerdane and R. Boscaino, "Origin of the visible absorption in radiation-resistant optical fibers," Opt. Mat. Express **3**(10), 1769–1776 (2013).
6. A. A. Witteles, "Neutron radiation effects on MOSFETs: theory and experiment", IEEE Trans. Nucl. Sci. **15**(6), 126–132 (1968).
7. S. Agnello, R. Boscaino, M. Cannas and F. M. Gelardi, "Instantaneous diffusion effect on spin-echo decay: experimental investigation by spectral selective excitation," Phys. Rev. B **64**(17), 174423 (2001).
8. P.V. Chernov, "Spectroscopic manifestations of self-trapped holes in silica," Phys. Stat. Sol. **B115**, 663–675 (1989).
9. E. Regnier, I. Flammer, S. Girard, F. Gooijer, F. Achten and G. Kuyt, "Low-dose radiation-induced attenuation at infrared wavelengths for P-doped, Ge-doped and pure silica-core optical fibres," IEEE Trans. Nucl. Sci. **54**(4), 1115–1117 (2007).
10. L. Skuja, T. Suzuki and K. Tanimura, "Site-selective laser spectroscopy studies of the intrinsic 1.9 eV luminescence center in glassy SiO_2," Phys. Rev. B **52**(21), 15208–15216 (1995).
11. L. Vaccaro, M. Cannas, S. Girard, A. Alessi, A. Morana, A. Boukenter, Y. Ouerdane, and R. Boscaino, "Influence of fluorine on the fiber resistance studied through the nonbridging oxygen hole center related luminescence," J. Appl. Phys. **113**, 193107 (2013).
12. M. Cannas and F.M. Gelardi, "Vacuum ultraviolet excitation of the 1.9 eV emission band related to nonbridging oxygen hole centers in silica," Phys. Rev. B **69,** 153201 (2004).
13. P. Martín, M. León and A. Ibarra, "Photoluminescence in neutron irradiated fused silica," Phys. Stat. Sol. **C2**(1), 624–628 (2005).
14. L. Skuja, "Optically active oxygen-deficiency-related centers in amorphous silicon dioxide," J. Non-Cryst. Solids **239,** 16–48 (1998).
15. R. A. Weeks, "Paramagnetic resonance of lattice defects in irradiated Quartz," J. Appl. Phys. **27,** 1376–1381 (1956).
16. T.-E. Tsai and D.L. Griscom, "On the structures of hydrogen-associated defect centers in irradiated high-purity a-SiO_2:OH," J. Non-Cryst. Solids **91** (2), 170–179 (1987).
17. E. J. Friebele, D. L. Griscom and M. Stapelbroek, "Fundamental defect centers in Glass: the peroxy radical in irradiated, high-purity, fused silica," Phys. Rev. Lett. **42**(20), 1346–1349 (1979).
18. M. Stapelbroek, D.L. Griscom, E.J. Friebele and G.H. Sigel Jr., "Oxygen-associated trapped-hole centers in high-purity fused silica," J. Non-Cryst. Solids **32**(1-3), 313–326 (1979).
19. K. Kajihara, M. Hirano, L. Skuja and H. Hosono, "Role of interstitial voids in oxides on formation and stabilization of reactive radicals: interstitial HO_2 radicals in F_2-laser-irradiated amorphous SiO_2," J. Am. Chem. Soc. **128**, 5371–5374 (2006).
20. L. Vaccaro, M. Cannas, and R. Boscaino, "Luminescence features of nonbridging oxygen hole centres in silica probed by site-selective excitation with tunable laser," Solid State Commun. **146,** 148–151 (2008).
21. L. Skuja, "Optical properties of defects in silica," in *Defects in SiO_2 and related dielectrics: Science and Technology*, G. Pacchioni, L. Skuja and D. L. Griscom ed. (Kluwer Academic Publishers, 2000).
22. M. Bredol, D. Leers, L. Bosselaar and M. Hutjens, "Improved model for OH absorption in optical fibers," J. Lightw. Technol. **8**(10), 1536–1539 (1990).
23. H. Imai and H. Hirashima, "Intrinsic and extrinsic defect formation in silica glasses by radiation," J. Non-Cryst. Solids **179,** 202–213 (1994).
24. H. Nishikawa, R. Nakamura, Y. Ohki and Y. Hama, "Correlation of preexisting diamagnetic defect centers with induced paramagnetic defect centers by ultraviolet or vacuum-ultraviolet photons in high-purity silica glasses," Phys. Rev. B **48**(21), 15584–15594 (1993).
25. F. Messina and M. Cannas, "In situ observation of the generation and annealing kinetics of E′ centres induced in amorphous SiO_2 by 4.7 eV laser irradiation," J. Phys.: Condens. Matter **17,** 3837–3842 (2005).
26. H. Hosono, Y. Ikuta, T. Kinoshita, K. Kajihara and M. Hirano, "Physical disorder and optical properties in the vacuum ultraviolet region of amorphous SiO_2," Phys. Rev. Lett. **87**(17), 175501 (2001).
27. L. Vaccaro, M. Cannas, B. Boizot and A. Parlato, "Radiation induced generation of non-bridging oxygen hole center in silica: intrinsic and extrinsic processes," J. Non-Cryst. Solids **353**, 586–589 (2007).
28. K. Kajihara, L. Skuja, M. Hirano and H. Hosono, "Role of mobile interstitial oxygen atoms in defect processes in oxides: interconversion between oxygen-associated defects in SiO_2 glass," Phys. Rev. Lett. **92**(1), 015504 (2004).
29. B. Brichard, P. Borgermans, A. Fernandez Fernandez, K. Lammens, and M. Decréton, "Radiation effect in silica optical fiber exposed to intense mixed neutron-gamma radiation field," IEEE Trans. Nucl. Sci. **48**(6), 2069–2073 (2001).
30. M. Vitiello, N. Lopez, F. Illas and G. Pacchioni, "H_2 crackong at SiO_2 defect centers," J. Phys. Chem. A

#230868 - $15.00 USD Received 27 Jan 2015; revised 11 Mar 2015; accepted 17 Mar 2015; published 30 Mar 2015

2000(104), 4674–4684 (2000).
31. L. N. Skuja, A. N. Streletsky and A. B. Pakovich, "A new intrinsic defect in amorphous SiO_2: twofold coordinated silicon," Solid State Commun. **50**(12), 1069–1072 (1984).

1. Introduction

Optical fibers are more and more used in harsh environments because of their data multiplexing and sensing capabilities. It is well known that radiations affect the fiber transmission properties depending on fiber composition, irradiation temperature, total dose, dose-rate and nature of radiation [1]. As a consequence, several works deal with the fiber response under γ-rays and characterize the induced point defects by using different spectroscopic techniques. The main centers present in the silica-based optical fibers are the same of fused silica [2]: the E′ center consists of a threefold coordinated silicon ($\equiv$Si$^\bullet$, where $\equiv$ represents the three bonds with three O atoms and $^\bullet$ is an unpaired electron); the nonbridging oxygen hole center (NBOHC) is a dangling oxygen bond ($\equiv$Si-O$^\bullet$); the peroxy linkage (POL) is a vacancy of silicon ($\equiv$Si-O-O-Si$\equiv$); the peroxy radical (POR) consists of a Si atom linked to an oxygen molecule with an unpaired electron delocalized on the two O atoms ($\equiv$Si-O-O$^\bullet$); the neutral oxygen vacancy ($\equiv$Si-Si$\equiv$); the twofold coordinated silicon consists of a Si coordinated with two O atoms and having a lone pair (=Si$^{\bullet\bullet}$, where $^{\bullet\bullet}$ represents two paired electrons in the same orbital).

On the contrary, the neutrons effects, present in civil nuclear applications as nuclear power plants, are the center of attention of fewer studies. Most of them focused on on-line measurements of radiation-induced attenuation (RIA). Cheymol et al. [3] showed a decrease in the RIA growth rate in the IR region during irradiation, without any saturation up to a fluence of 10^{20} n/cm^2 and a γ-dose of 16 GGy. Moreover, the authors observed a recovery between two successive irradiation cycles, due to the thermal annealing, and a fast RIA increase up to the value reached before stopping the previous irradiation period, at the subsequent cycle. They explained this behavior with an annealing-induced detrapping and a subsequent radiation-induced re-trapping of the charge carriers from the defect sites. The not high temperature held inside the reactor (around 30°C) does not permit to remove the defect sites themselves. Brichard et al. [4], instead, studied the RIA in the visible spectral region, by comparing the effects of only γ-rays (at 0.5 MGy) and mixed γ-rays and neutrons (at 3.3 MGy γ-dose and the fluence of about 6×10^{17} n/cm^2). The decomposition as a sum of Gaussian bands, on the basis of previous studies, resulted in the same optical parameters for both kinds of irradiations.

Detailed studies on absorbing, photo-luminescent or paramagnetic defects were realized on neutron-irradiated bulk-silica; but these results cannot be easily extended to the optical-fibers, since the radial distribution of dopants and strain inside the fiber influences the defects formation. As a consequence, the microscopic processes originating the defects induced on optical fibers by neutrons are not clear.

In this paper, we compare the effects induced on a Fluorine-doped multi-mode radiation resistant fiber by γ-rays, up to a dose of 10 MGy(SiO_2), and neutrons, up to a fluence of 10^{17} n/cm^2. By combing complementary spectroscopic techniques, as radiation-induced attenuation (RIA), confocal micro-luminescence (CML), time-resolved photo-luminescence and electron paramagnetic resonance (EPR), we determine the concentrations and cross-section distribution of defects inside the fiber, highlighting the similarities and differences between γ-ray and neutron irradiations.

2. Experimental details

We tested a fluorine-doped silica multi-mode graded index fiber with acrylate coating. The diameters of core and cladding are 50 μm and 125 μm, respectively. The F-content ranges from about 0.2 wt% at the core center to 5 wt% in the cladding.

#230868 - $15.00 USD Received 27 Jan 2015; revised 11 Mar 2015; accepted 17 Mar 2015; published 30 Mar 2015

Two kinds of irradiations, pure γ-rays and mixed γ-rays and neutrons, were realized on these fibers. The γ-ray irradiations were performed with a ^{60}Co source in the Brigitte underwater-γ-irradiation-facility in SCK-CEN (Mol, Belgium). The dose-rate and the irradiation temperature can be varied between 3 and 8 Gy/s and 20 and 60°C, respectively, by changing the sample-relative-position to the source. In such a way, we can obtain samples with different accumulated doses, up to 10 MGy, for a same irradiation duration and run. The mixed γ-rays and neutrons irradiations were performed at the pool-type reactor TRIGA Mark II of the CNESTEN (Maamoura, Morocco). The neutron flux and the γ-dose-rate are about 2×10^{12} n/(cm^{2}s) and 40 Gy/s, respectively. The irradiation temperature is lower than 50°C. The neutron fluence varies between 10^{15} n/cm^2 and 10^{17} n/cm^2, with an accumulated γ-dose between 0.02 and 2 MGy. It is known that the secondary ionization effects induced by a neutron fluence of 2×10^{12} n/cm^2 are equivalent to a γ-dose of 1 Gy(SiO_2) [6]. As a consequence, e.g. the highest fluence of 10^{17} n/cm^2 causes the same damages, for secondary ionization, as a γ-dose of 5×10^{-2} MGy, which is two orders of magnitude lower than the γ-dose associated with that neutron fluence, i.e. about 2 MGy. Hence, the neutron-induced secondary ionization effects can be negligible with respect to the γ-induced ones. Complementary spectroscopic techniques were used to study, ex situ, the permanent defects induced by pure γ-rays or mixed γ and neutrons irradiation. The measurements were performed some months after irradiation, at room temperature (RT).

Spectral attenuation measurements were carried out by the cut-back method. All the transmission spectra were recorded by using two white light sources and two spectrometers from Ocean Optics: the QE65000 for the visible range, between 400 and 800 nm, and the NIR-Quest for the IR range, between 900 and 2100 nm.

Photoluminescence (PL) spectra emitted from different zones of the fiber-transverse-section were acquired through confocal microspectroscopy by a LabRam Aramis (Jobin-Yvon/Horriba) spectrometer equipped with a He-Cd ion laser emitting at 3.82 eV (325 nm) and a He-Ne laser emitting at 1.96 eV (633 nm), a charge coupled device (CCD) camera and 3D-microtranslation stages. The spatial resolution was fixed at 3 μm for the UV excitation, through a $\times$40 objective and a confocal-hole-diameter of 50 μm, and at 1.5 μm for the visible excitation, by using a $\times$100 objective and the same confocal-hole. Thanks to the time resolved photoluminescence set-up and its UV excitation system, realized by an optical parametric oscillator pumped by the third harmonic (3.50 eV – 355 nm) of a Nd:YAG laser (pulse width of 5 ns, repetition rate of 10 Hz) and a II harmonic generation nonlinear crystal, all the PL bands, even those non-observable with the confocal microscopy system, were studied and lifetime measurements were performed. The laser beam was focused into the core of a stripped piece of fiber. The emitted light was spectrally resolved by a 500 nm blazed grating with 300 grooves mm^{-1}. Spectra were acquired by a gated intensified CCD camera driven by a delay generator, setting the acquisition time width Δt during which the CCD is enabled to reveal the light, and the delay T_D of the acquisition with respect to the laser pulse arrival.

Finally, the presence of paramagnetic defects was investigated by recording EPR spectra at RT and 77 K through a Bruker EMX-Micro Bay spectrometer working at 9.8 GHz with a magnetic-field modulation frequency of 100 kHz. The microwave power was varied between 200 nW and 200 mW to put in evidence the different defects. Each recorded spectrum was normalized by the sample mass and some experimental parameters (i.e. acquisition time and power). The absolute concentration of defects was estimated by comparing the double integral of the normalized EPR spectrum with that of a reference sample, an irradiated bulk silica sample whose E′ concentration was already known [7]. The relative error on the concentrations of the different types of defects is about 20%, whereas that on the absolute concentration is about 50%.

#230868 - $15.00 USD Received 27 Jan 2015; revised 11 Mar 2015; accepted 17 Mar 2015; published 30 Mar 2015

3. Results and discussion

3.1. Radiation induced attenuation

Figure 1 displays RIA spectra as a function of the γ-ray dose and the neutron fluence. All the curves present a similar trend: an absorption band around 620 nm, an UV-tail, which increases with decreasing wavelength above 480 nm, and an IR-tail that increases with increasing wavelength. The RIA intensity increases with the γ-dose and the neutron fluence.

To highlight the neutron-induced effects in the visible range, we compare the RIA bands of the samples irradiated at 10^{17} n/cm^2 and at 3 MGy. The γ-dose associated with the neutron fluence of 10^{17} n/cm^2 is higher than 2 MGy, according to the dose equivalence, and so comparable with the γ-dose of the 3 MGy irradiated sample. Firstly, we note in Fig. 1 that the attenuation at 620 nm (2 eV) is higher for the neutron-irradiated sample: 2.9 dB/m at the γ-dose of 3 MGy and 8.23 dB/m at the neutron fluence of 10^{17} n/cm^2, three times greater. Secondly, we observe in Fig. 2 a band-shape change in the neutron irradiated samples for fluences higher than 10^{15} n/cm^2. We have already demonstrated that the asymmetric band centered at 2 eV (FWHM of about 0.4 eV), observed in the γ-irradiated F-doped fiber, does not change its shape with increasing γ-dose up to 10 MGy and it is associated with an only defect, the non-bridging-oxygen-hole center (NBOHC) [5]. This change of the 2 eV absorption band could be attributed to an inhomogeneous widening of the NBOHC band (increase of the FWHM of about 17%) or to the presence of another contribution at higher energies, around 2.6 eV.

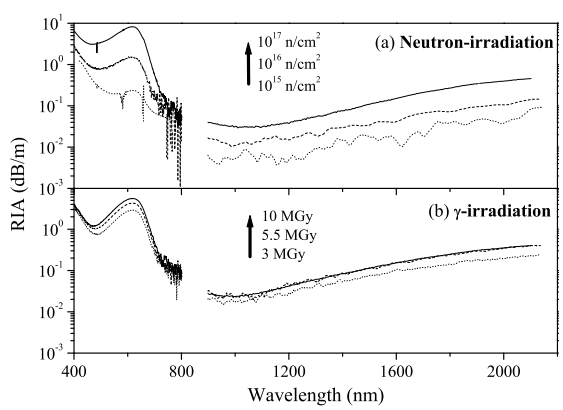

Fig. 1. RIA spectra of the multimode F-doped fiber irradiated at (a) three neutron fluencies and (b) three γ-ray doses.

In the IR range, the RIA is at least one order of magnitude lower than the absorption at 2 eV; indeed, for both maximum irradiation levels, the RIA increases up to 0.06 dB/m at 1.3 μm and 0.11 dB/m at 1.55 μm. Regarding the IR contribution, few studies are devoted to the identification of its origin. Chernov [8] was the first to assign an IR band peaked at wavelengths longer than 1500 nm to Self-Trapped Holes (STHs). Subsequently, Regnier et al. [9] related with the same defect their absorption band peaked around 1800 nm and observed in γ-irradiated single-mode fibers at a 100 Gy dose. In contrary with the work of Regnier et al., we did not take into account the wavelength dependency of the mode power fraction, which can influence the absorption band shape. As a consequence, we cannot, in our case, attribute the IR absorption to a defect with known structure.

#230868 - $15.00 USD Received 27 Jan 2015; revised 11 Mar 2015; accepted 17 Mar 2015; published 30 Mar 2015

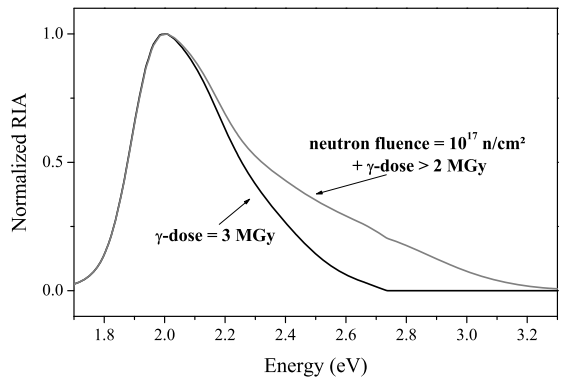

Fig. 2. Normalized absorption band at 2 eV of two samples irradiated at the neutron fluence of 10^{17} n/cm^2 (grey line) and at the γ-dose of 3 MGy (black line). These bands were obtained by subtracting the UV contribution to the RIA curves.

3.2. Photoluminescence

Thanks to the CML technique, we studied the photo-luminescent defects under UV excitation (3.82 eV - 325 nm). Figure 3 reports the PL bands observed in the γ- and neutron-irradiated samples at the highest doses.

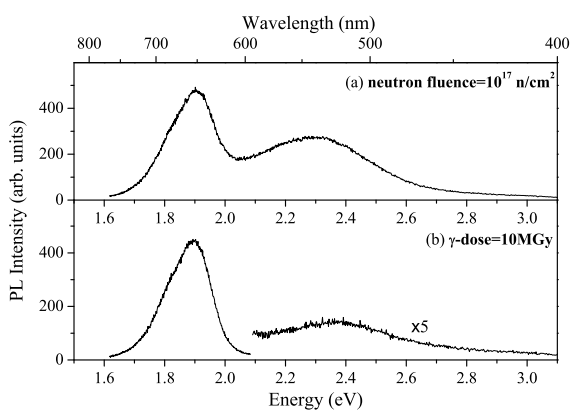

Fig. 3. PL spectra emitted from the core center of the fiber irradiated at (a) the neutron fluence of 10^{17} n/cm^2 and (b) the γ-dose of 10 MGy; excitation at 3.82 eV (325 nm).

In all the samples, irradiated or not, the PL spectra show an asymmetric band peaked at 1.9 eV (FWHM of about 0.17 eV), associated in literature with the NBOHCs [10]; whereas other PL bands in the green region of the spectrum (consequently hereafter named green bands) appear depending on the irradiation type and level:

- in pristine and irradiated samples with γ-rays up to a 10 MGy dose or neutron fluences lower than 10^{16} n/cm^2, the green band is peaked around 2.35 eV (FWHM of 0.54 eV) and its intensity is very low compared to that of NBOHC (i.e. only the 5% for the 10 MGy irradiated fiber);

#230868 - $15.00 USD Received 27 Jan 2015; revised 11 Mar 2015; accepted 17 Mar 2015; published 30 Mar 2015

- at higher neutron fluences, another band peaking at lower energy (around 2.28 eV, FWHM of 0.47 eV) appears, with intensity of the same order of magnitude as that of the NBOHC contribution.

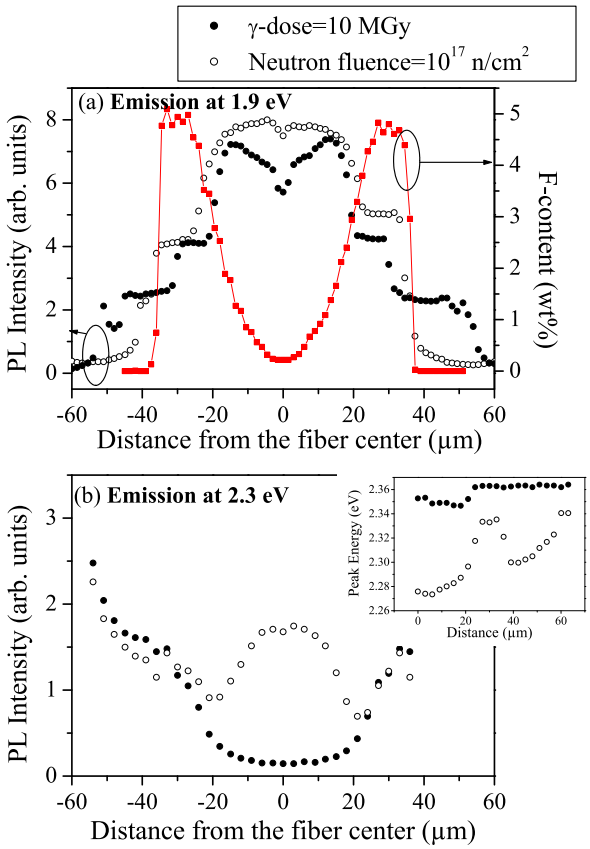

Fig. 4. PL band profiles along the diameter for the fiber irradiated at 10^{17} n/cm^2 (empty circles) and at 10 MGy (full circles): (a) emission at 1.9 eV (650 nm) under excitation at 1.96 eV (633 nm) and F-profile (full red squares); (b) PL intensity at 2.3 eV (540 nm) under excitation at 3.82 eV (325 nm). The inset shows the peak energy of the green band as a function of the distance from the fiber center.

For the fibers irradiated at the highest γ-dose and neutron fluence, the intensity-distribution of these PL bands along the fiber diameter is shown in Fig. 4. The contribution at 1.9 eV was isolated by using the excitation energy at 1.96 eV (He-Ne laser line). The distribution of the NBOHCs along the fiber diameter does not change significantly for the sample irradiated with a 10^{16} n/cm^2 neutron fluence or with γ-rays (curves not shown here), whereas it changes at the highest neutron fluence, as displayed in Fig. 4(a). For the samples irradiated with γ-rays or with low neutron fluences, the NBOHC distribution depends on the Fluorine content, as already demonstrated [11]. For this neutron-irradiated sample the photo-luminescent centers are mainly present in the core; in the cladding their concentration rapidly decreases to zero towards the outside part of the fiber.

In the case of the neutron-irradiated samples at fluences higher than 10^{15} n/cm^2, the green band consists of two contributions whose interplay in the core and in the cladding is evident

#230868 - $15.00 USD Received 27 Jan 2015; revised 11 Mar 2015; accepted 17 Mar 2015; published 30 Mar 2015

by the comparison between the two samples in Fig. 4(b). It seems clear that the 2.28 eV band typical of neutron-irradiation is present only in the fiber core, indeed its peak shifts towards higher energies along the fiber diameter from the center outwards, as shown in the inset.

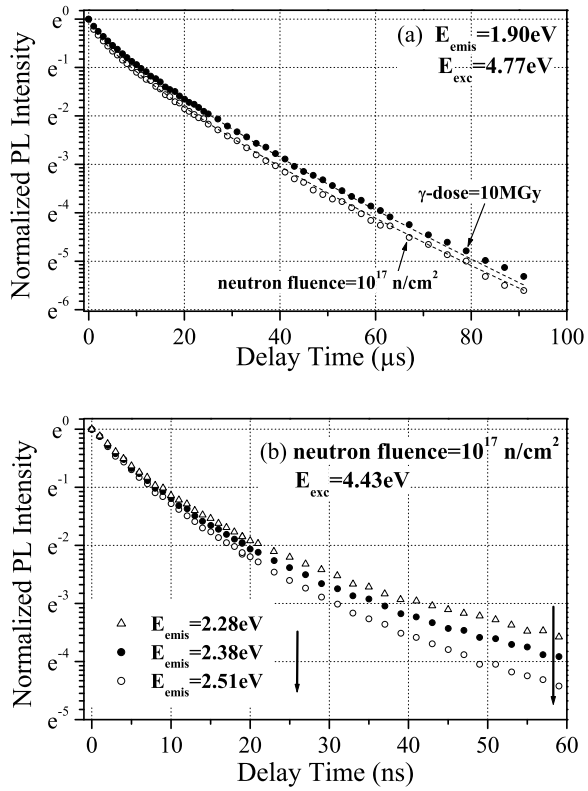

Fig. 5. (a) Semilog plot of the PL decay measured at 1.9 eV (650 nm) in the samples irradiated at 10^{17} n/cm^2 (empty circles) and at 10 MGy (full circles), under excitation at 4.77 eV (260 nm). The dashed lines represent the best-fitting stretched exponential functions. (b) Semilog plot of the PL decay excited at 4.43 eV (280 nm) in the neutron-irradiated fiber at the fluence of 10^{17} n/cm^2 and measured at three different energies: 2.28 eV (545 nm – empty triangles), 2.38 eV (521 nm - full circles) and 2.51 eV (494 nm - empty circles).

The PL-lifetime was studied by recording time resolved PL spectra at different delays T_D and acquisition-time widths Δt. The 1.9 eV PL decay was obtained carrying out time resolved PL spectra on increasing T_D up to 90 μs with Δt ranging between 1 and 4 μs, under excitation at 4.77 eV (260 nm), that is the maximum of its excitation spectrum [12]. The decay curves monitored at $E_{emis} = 1.9$ eV in the γ- or neutron-irradiated samples are compared in Fig. 5(a): both agree with a stretched exponential $\exp\left(-(t/\tau)^{\beta}\right)$ but are characterized by different values of lifetime τ and stretching parameter β, as reported in the following table.

The time decay of the band around 2.3 eV present in the neutron-irradiated sample is almost completed over 60 ns; therefore, the time resolved PL spectra were recorded by increasing T_D up to 60 ns with Δt ranging between 1 and 2 ns, under excitation at 4.43 eV (280 nm). This defect shows inhomogeneity properties; indeed, the emission peak energy shift is accompanied

#230868 - $15.00 USD Received 27 Jan 2015; revised 11 Mar 2015; accepted 17 Mar 2015; published 30 Mar 2015

Table 1. Parameters characterizing the PL decay of the NBOHCs.

Irradiation	Lifetime τ (μs)	Stretching parameter β
10 MGy	10.7 ± 0.6	0.80 ± 0.02
10^{17} n/cm^2	9.0 ± 0.7	0.74 ± 0.04

by an emission lifetime change (Fig. 5(b)). All the decay curves of Fig. 5(b) are described by the sum of two exponential functions: the fastest component has a lifetime of about 5 ns and the slowest one of 20 ns. The origin of this band is still unknown. A band peaked around 2.3 eV (FWHM of about 0.5 eV) has been observed by Martin et al. [13] in silica bulk samples irradiated with neutrons at fluences higher than 10^{17} n/cm^2. Since they reported the excitation of this PL, consisting of two bands peaked at 4.6 eV (FWHM of 0.6 eV) and 3.9 eV (FWHM of 0.64 eV), we decided to study its decay by exciting this PL near the maximum of its excitation spectrum, 4.43 eV. We can infer that, since the lifetime is in the nanosecond domain, this PL has to be related with an allowed transition between two states having the same spin of an intrinsic defect induced by irradiation with particles, as neutrons.

Concerning the other PL band around 2.35 eV, the time-resolved photoluminescence set-up does not allow us to observe it; in comparison with this, the CML system is very powerful to detect bands having low intensity.

Finally, thanks to the excitation system of the time-resolved photoluminescence set-up, the presence of another diamagnetic defect was highlighted in all the irradiated samples, independently of the irradiation type: this is the two-fold coordinated silicon. This defect gives rise to an absorption band at 5.05 eV and two luminescence bands, corresponding to the transition from the singlet and triplet excited states [14]: the fast component (lifetime of about 4 ns) is peaked at 4.34 eV, with FWHM of 0.55 eV, whereas the slow component (lifetime of 10 ms) is peaked at 2.64 eV, with FWHM of 0.40 eV. Figure 6 reports the time-resolved PL spectra detected in different time windows under excitation at 5.06 eV (245 nm), to evidence the two contributions.

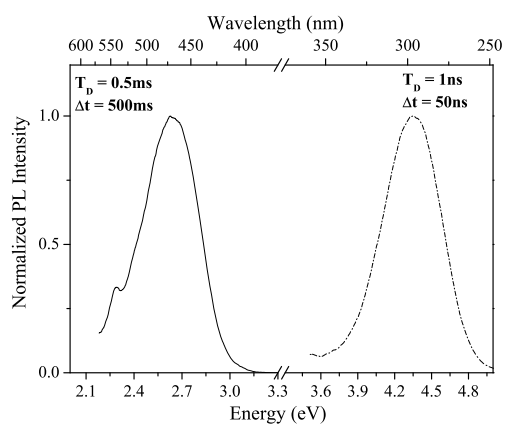

Fig. 6. Normalized time-resolved PL spectra of the sample irradiated at 10^{17} n/cm^2 measured under laser excitation at 5.06 eV (245 nm) in different time windows. For the fast component peaked at 4.34 eV (dashed line), T_D=1 ns and Δt=50 ns. For the slow component peaked at 2.64 eV (continuous line), T_D=0.5 ms and Δt=500 ms.

#230868 - $15.00 USD Received 27 Jan 2015; revised 11 Mar 2015; accepted 17 Mar 2015; published 30 Mar 2015

3.3. *Electron paramagnetic resonance*

Figure 7 shows the EPR signals observed in the irradiated samples, regardless of the kind of irradiation. The most common paramagnetic intrinsic defect is the E′ center [15], whose EPR spectrum (Fig. 7(a)) is recorded at RT with a microwave power of 0.8 μW and a modulation amplitude of 0.1 G. A doublet of lines centered on the E′ signal with a magnetic field separation of 74 G was recorded at RT with a microwave power of 0.2 mW and a modulation amplitude of 1 G and is reported in Fig. 7(b). It is associated with a variant of the E′ center, named H(I) center [16]: it is due to the hyperfine interaction between the unpaired electron and the nucleus of a H atom substituting a neighboring O of the dangling Si bond. In contrast to these two centers, the oxygen-related defect signals [17, 18] are very large and they overlap at RT; therefore, to separate the different contributions, EPR spectra were recorded at 77 K, with a microwave power of 1 mW and a modulation amplitude of 0.6 G. We compared the signal shape with a linear combination of the two curves reported by Kajihara et al. [19] associated with POR and NBOH centers, to separate the two contributions. The defects concentration was calculated as above explained.

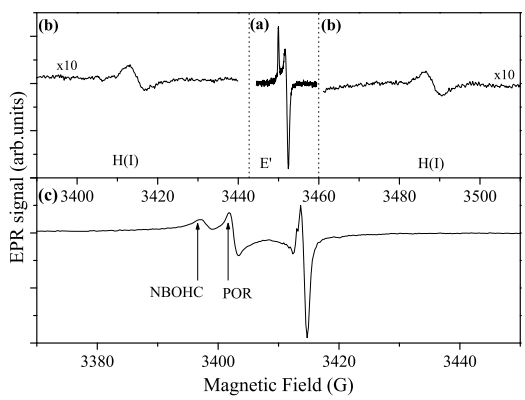

Fig. 7. EPR spectra recorded in the 10 MGy irradiated sample with different values of microwave power (P) and modulation amplitude (H_m) to put in evidence the different defects. (a) Spectrum of the E′ center acquired at RT, with $P = 0.8$ μW and $H_m = 0.1$ G. (b) Doublets of 74 G typical of the H(I) centers acquired at RT with $P = 0.2$ mW and $H_m = 1$ G. (c) Oxygen-related defect signals recorded at low temperature, 77 K, with $P = 1$ mW and $H_m = 0.6$ G.

The average values of the paramagnetic defects concentrations are reported in Fig. 8, which highlights that:

- before irradiation, the sample is characterized by an E′ concentration of about 10^{14} cm^{-3} whereas all the other defects have an undetectable concentration;
- the concentration of all the defects grows with both γ-dose and neutron fluence;
- the E′ concentration reached at the highest γ-dose and at the highest neutron fluence is about 10^{17} cm^{-3}, three orders of magnitude higher than in the pristine sample;
- regardless of the kind of irradiation, there is a larger production of E′ than NBOHCs or PORs.

#230868 - $15.00 USD Received 27 Jan 2015; revised 11 Mar 2015; accepted 17 Mar 2015; published 30 Mar 2015

We have to note that the EPR set-up gives a value of the defects concentration averaged over all the volume, consisting of core and cladding, independently of the real distribution of the centers. Combining this technique with the CML, the concentration profile along the fiber diameter can be calculated for the defects that are both paramagnetic and photo-luminescent, such as the NBOHCs.

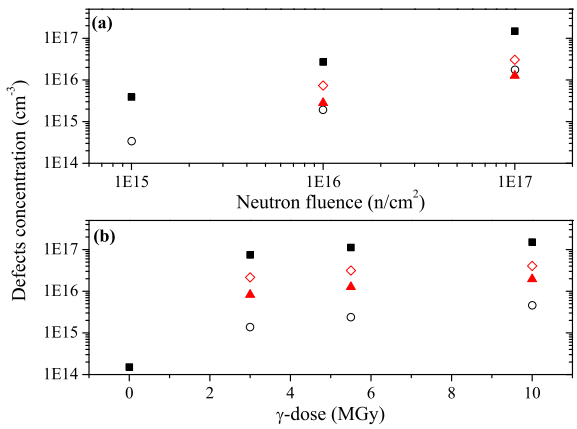

Fig. 8. Defects concentration as a function of (a) the neutron fluence and (b) the γ-dose: E′ centers - full squares; H(I) centers - empty circles; NBOHCs - empty diamonds; PORs - full triangles.

Moreover, assuming that the signal at 2 eV (about 600 nm) propagates inside the core of the multi-mode fiber, the concentration of the NBOHCs present inside the fiber core (N_{core}) can be estimated by the RIA measurements through Smakula's formula and the oscillator strength value (that is about 1.9×10^{-4} at 2 eV [20]), according to the following expression:

$$N_{core}^{OA} = 3.3 \times 10^{16} \times OA(2eV) \left[\mathrm{cm}^{-3}\mathrm{dB/m}^{-1}\right] \tag{1}$$

where OA(2eV) indicates the intensity of the absorption band at 2 eV, expressed in dB/m. Figure 9 compares the values of the NBOHC concentration in the core calculated by the RIA results with those obtained combining both EPR and CML. With the exception of the point corresponding to the highest neutron fluence, the graph clearly highlights a linear correlation existing for all the samples: the concentration value obtained by EPR spectra is systematically smaller by a factor 2, which is reasonable considering the error of 50% on the absolute estimation of the concentration through the EPR measurements. At the fluence of 10^{17} n/cm^2, the core concentration obtained by the absorption measurements increases by a factor of about 1.5 with respect to the linear trend. This can be due to an overestimation of the OA concentration or an underestimation of the EPR value. No experimental data supports this latter hypothesis. On the contrary, thanks to the time-resolved PL set-up a 15% reduction of the NBOHC lifetime was observed at RT for the highest neutron fluence. As a consequence, an overestimation of the concentration obtained by the absorption measurements could be explained by an underestimation of the oscillator strength (f). Indeed, f is inversely proportional to the lifetime measured at low temperature (LT) [21] and a reduction of the lifetime will provide an increase of the f value. This could be due to modifications of the environment around the defect, even if Raman spectra (not shown here) highlighted no structural change in the silica network.

#230868 - $15.00 USD Received 27 Jan 2015; revised 11 Mar 2015; accepted 17 Mar 2015; published 30 Mar 2015

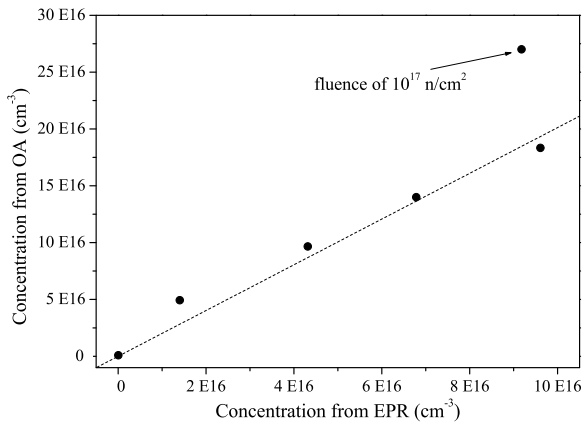

Fig. 9. Correlation between the values of the NBOHC concentration in the core, calculated by the RIA at 2 eV through equ. 1, as a function of those obtained by combining EPR and CML measurements. The dashed line represents the linear best fitting obtained without taking into account the point corresponding to the highest neutron fluence (the correlation coefficient is R = 0.968).

3.4. Generation processes

In this section we discuss the generation processes of defects, on the basis of the large literature on this subject.

It is important to note that the pristine samples are characterized by an OH concentration of about 0.2 ppm, i.e. 5×10^{15} cm^{-3}, which corresponds to a 1.39 μm absorption lower than 0.01 dB/m [22]; unfortunately, this is too low to be appreciated by our RIA measurements and, as a consequence, no radiation-induced variation of the OH groups is observable.

As shown in Fig. 8, most of defects induced by γ-rays or neutrons are E′ centers. The main cause is the presence of more precursors [23]; however, our measurements were performed some months after irradiation and the E′ centers are involved in less recombination processes with respect to the oxygen-related defects. The precursors of E′ centers are:

- oxygen-deficient centers, as neutral oxygen vacancies [24], whose presence is conceivable from that of the twofold coordinated centers;
- Si-H bonds [25], whose presence has not been demonstrated here by evidences;
- strained Si–O–Si bonds, whose cleavage generates a couple E′ – NBOHC [26].

Precisely, the strained bonds are the main precursors of the NBOHCs; indeed, they can be also created by the radiolysis of the ≡Si-O-H bonds [27], but the concentration value of the OH bonds before irradiation is one order of magnitude lower than that of the radiation-induced NBOHCs. The precursors of PORs are the peroxy linkages or an E′ with an O_2 molecule [28]. Since there is no evidence of their presence before irradiation, maybe the precursors may be themselves induced by the radiation.

Finally, the H(I) centers can be created by two possible reactions:

- the first consists of the trapping of an H atom by an ODC(II) [16], whose presence in the irradiated samples has been demonstrated with the time-resolved photoluminescence;

#230868 - $15.00 USD Received 27 Jan 2015; revised 11 Mar 2015; accepted 17 Mar 2015; published 30 Mar 2015

- the second consists of the breaking of a Si-O bond of a silicon atom linked to three binding O and a H, but no evidence of the Si-H bonds has been observed.

It is worth noting that the H(I) concentration is of the same order of magnitude of the OH concentration, up to a γ-dose of 10 MGy and a neutron fluence of 10^{16} n/cm^2. At the highest neutron fluence, instead, the H(I) defect concentration increases by a factor 4. This result suggests an increase of the amount of H atoms inside the optical fiber due to the neutrons effect on the acrylate coating. Neutron knock-on produces recoil protons from the coating that diffuse in the fiber glass, as reported by Brichard et al. [29].

Figure 10 highlights a linear correlation between the concentrations of the oxygen related defects and the E′ centers, thus suggesting the same dependence on the dose for the generation processes of these defects. However, the point associated with the highest neutron fluence deviates from this correlation: for the same E′ concentration induced by the 10 MGy dose, less NBOHCs and PORs seem to be generated by the fluence of 10^{17} n/cm^2. On the basis of the increase of H concentration at this fluence, we can state that more recombination processes occur for the oxygen related defects after irradiation. Indeed, it is well known that the H_2 molecule cracks spontaneously on a NBOHC whereas on E′ centers the formation of Si-H and neutral H atom has an activation energy of less than 0.5 eV [30]. This hypothesis is confirmed by the results of Fig. 4(a), where a lower NBOHC concentration in the outer part of the cladding is shown for the fiber irradiated at the highest neutron fluence with respect to the others: for that particular fiber, the induced NBOHCs in the outer part of the cladding recombine with the hydrogen atoms coming from the coating.

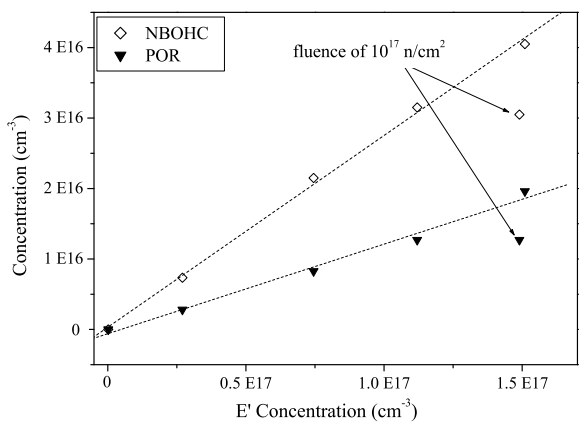

Fig. 10. Concentration of NBOHCs (empty diamonds) and PORs (full triangles), as a function of that of E′ centers.

In table 2 we summarize the most important spectroscopic characteristics of each observed center.

4. Conclusion

Complementary spectroscopic techniques, as RIA, PL and EPR, were combined to compare the effects on a Fluorine-doped multi-mode fiber of γ-rays, up to 10 MGy dose, and neutrons, up to a fluence of 10^{17} n/cm^2. The microscopic processes at the defects origin are the same for both kinds of irradiations, in the investigated dose ranges. The most abundant center is the E′, whose origin is related to pre-existent precursors. The NBOHCs are mainly produced from the cleavage of strained Si-O-Si bonds, whereas the precursors of the PORs are themselves induced

#230868 - $15.00 USD Received 27 Jan 2015; revised 11 Mar 2015; accepted 17 Mar 2015; published 30 Mar 2015

Table 2. List of all the defects detected in the samples irradiated at the highest doses (γ-dose of 10 MGy and neutron fluence of 10^{17} n/cm^2). The spectroscopic characteristics are also reported here (τ indicates the PL lifetime), whereas the concentration values are calculated with the EPR technique.

Defect		**E´**	**NBOHC**	**POR**	**two-fold coordinated Si**
Structure		≡Si$^\bullet$	≡Si-O$^\bullet$	≡Si-O-O$^\bullet$	=Si$^{\bullet\bullet}$
Techniques		EPR	OA PL EPR	EPR	PL
EPR concentration	γ	15	4.1	2.0	diamagnetic
(10^{16}cm^{-3})	γ-n	15	3.1	1.3	
OA	γ		OA at 2 eV $\sim$ 5.5 dB/m		OA at 5.05 eV [31]
	γ-n		$\sim$ 8.2 dB/m		
PL	γ	no signal	PL at 1.9 eV τ=10.7μs	no signal	for both irrad. PL at 4.34 eV ($\sim$4ns)
	γ-n		τ=9.0μs		PL at 2.64 eV ($\sim$10ms)
Defect		**H(I)**			
Structure		=Si$^\bullet$-H	unknown	unknown	
Techniques		EPR	PL	OA	
EPR concentration	γ	0.5	no signal	no signal	
(10^{16}cm^{-3})	γ-n	1.7			
OA			no signal	tail of OA in IR	
PL	γ	no signal	not observable	no signal	
	γ-n		PL at 2.28 eV $\tau_1 \sim$ 5ns; $\tau_2 \sim$ 20ns		

by the radiation. However, neutrons induce also an intrinsic peculiar defect, characterized by a photo-luminescence around 2.28 eV. This PL band has been already detected in neutron-irradiated silica bulks [13] and we have determined its lifetime. Moreover, the highest neutron fluence changes the spectroscopic properties of the 1.9 eV PL band associated with NBOHCs: a 15% reduction of its lifetime, from 11 μs to 9 μs, has been detected. This could suggest an increase of the oscillator strength of the transition at 2 eV as a consequence of the neutron effects on the fiber structure, since no change has been reported in literature on the silica bulk. Finally, an increase of the H(I) concentration and a reduction of the oxygen-related defects concentration confirm the introduction of hydrogen atoms from the acrylate coating due to knock-on processes induced by neutrons at high fluences (10^{17} n/cm^2, in our case).

As a conclusion, even if there is no difference in the microscopic processes at the defects' origin, a neutron fluence of 10^{17} n/cm^2 seems to start changing the spectroscopic properties of the defects, as we demonstrated for the NBOHC.

#230868 - $15.00 USD Received 27 Jan 2015; revised 11 Mar 2015; accepted 17 Mar 2015; published 30 Mar 2015